


## Noiseless and efficient quantum information transmission for fiber-based continuous-variable quantum networks

Jiliang Qin<sup>1,2</sup>, Jialin Cheng<sup>1,\*</sup>, Shaocong Liang<sup>1</sup>, Zhihui Yan<sup>1,2</sup>, Huadong Lu<sup>1,2,†</sup> and Xiaojun Jia<sup>1,2,‡</sup>

<sup>1</sup>State Key Laboratory of Quantum Optics and Quantum Optics Devices, Institute of Opto-Electronics, Shanxi University, Taiyuan 030006, People's Republic of China

<sup>2</sup>Collaborative Innovation Center of Extreme Optics, Shanxi University, Taiyuan 030006, People's Republic of China

 (Received 5 December 2023; revised 2 May 2024; accepted 20 May 2024; published 11 June 2024)

Quantum state transmission and quantum information transmission (QIT) through fiber channels hold immense promise for advancing the scope of quantum information applications. However, besides unavoidable transmission loss, channel noise accelerates the decoherence of quantum states and severely limits the transmission distance in practical continuous-variable quantum state transmission. To address the issue of channel noise in metropolitan quantum fiber-optic links, we propose a scheme called dual-channel transferring after interference. This scheme exhibits immunity to additional channel noise while maintaining sufficient communication capacity. Based on this scheme, we experimentally achieve the transmission of a  $-5.9$ -dB squeezed state at  $1.3\ \mu\text{m}$  through 3 km of optical fiber. We obtain a  $-3.2$ -dB output squeezed state and demonstrate that this decrease is solely attributable to channel loss, independent of channel noise. Incidentally, we achieve an improved measurement sensitivity of guided acoustic-wave Brillouin scattering noise in a fiber channel exploiting squeezed light. In addition, beyond its simplicity of installation and ease of operation, this approach also offers the highest transmission capacity compared with the existing QIT technologies. Our scheme is suitable for almost all modulation-free continuous-variable quantum information protocols, such as quantum secret sharing, quantum entanglement swapping, and some quantum key distribution schemes with entangled states, as well as participating in the construction of future quantum networks.

DOI: [10.1103/PhysRevApplied.21.064026](https://doi.org/10.1103/PhysRevApplied.21.064026)

### I. INTRODUCTION

A quantum network is one of the ultimate goals of quantum communication technologies. The interconnection of independent quantum computing systems, quantum sensing systems, and small-scale quantum communication systems through fiber-optic networks holds the potential to unlock more remarkable functions compared to individual quantum systems. Given the deterministic preparation of quantum state high-speed measurement capabilities, compatibility with classical fiber-optic networks, and cost-effectiveness, continuous-variable (CV) quantum information is well-suited to the construction of metropolitan quantum networks, especially in scenarios where node distances range from 2 to 50 km. The transmission of quantum information over fiber channels is crucial for many quantum communication applications, including quantum repeaters [1–3], quantum key distribution (QKD)

[4,5], quantum secret sharing [6], and quantum teleportation [7,8]. Balanced homodyne detection assisted by a strong and stable local oscillator (LO) is necessary in most fiber-based CV quantum communication protocols. However, channel noise, complex phase control, and limited channel capacity in the fiber are the main obstacles that limit the practical applications of these techniques.

An attempt to address these challenges involved an early CV-QKD experiment using two identical fiber channels for transmitting the signal light and LO [9]. Under the circumstances, serious phase noise in the two fibers imposed significant limitations on transmission distance and secret key rate. Generating the LO “locally” using an independent laser source at the receiver’s end with classical coherent communication techniques, such as feed-forward carrier recovery [10], optical phase-locked loops [11], and optical injection phase-locked loops [12], have been explored to reduce relative phase noise. However, the application to future quantum networks remains limited due to the weak quantum signal, the low tolerable phase noise, and the uneconomical setup. An independent laser source at the receiver’s end is also necessary in such a metropolitan

\*Corresponding author: [chengjl@sxu.edu.cn](mailto:chengjl@sxu.edu.cn)

†Corresponding author: [luhuadong@sxu.edu.cn](mailto:luhuadong@sxu.edu.cn)

‡Corresponding author: [jiaxj@sxu.edu.cn](mailto:jiaxj@sxu.edu.cn)

CV QKD. Other excellent technology for a locally generated LO is the pilot-aided feed-forward data-recovery scheme, in which both the quantum signal and a strong phase-reference pulse are transmitted [13]. This scheme enables reliable coherent detection and suppresses phase noise between the signal field and a locally generated LO, meeting QKD requirements. However, the advantages are not significant due to an additional signal reference and necessary laser for the “locally” LO in some QKD schemes based on CV entangled states [14].

Achieving a highly stable relative phase between the signal light and LO by transmitting them through the same fiber has proven effective in a CV-QKD experiment, though this transmission method will introduce guided acoustic wave Brillouin scattering (GAWBS) photons from the strong LO on the signal field and leads to an increase in channel noise. This approach, employing time multiplexing, demonstrated a secure key rate of 2 kbits/s over a 25-km fiber channel [15]. In a subsequent experiment, a secure key rate of 30 kbits/s was achieved over 5 km of fiber using frequency and time multiplexing [16]. To further enhance the transmission performance, polarization-time-division multiplexing (PTDM) was employed for CV quantum communication, where the LO was modulated, effectively reducing mutual interference between the signal light and LO [17,18]. However, modulating the LO can reduce insertion loss of the signal field but still generate extra noise and reduce channel capacity due to pulse modulation. Especially in the case that the continuous-light field needs to be transmitted, for example, in some deterministic quantum secret sharing [19], quantum entanglement swapping [20,21], and QKD [14] schemes, the entangled state and LO fields are expected to be continuous for a higher communication capacity and detecting finer signal variations. By reducing the LO power to reduce the GAWBS noise caused by polarization-division multiplexing (PDM), deterministic quantum teleportation through fiber channels can be realized, but the transmission distance is limited [8].

In brief, the channel capacity and the presence of channel noise are critical factors that determine the achievable communication rate and transmission distance in quantum communication, particularly in CV quantum state transmission and quantum information transmission (QIT). Regrettably, the simultaneous influence of phase fluctuations and GAWBS noise in the fiber makes it challenging to achieve both a high communication capacity and noise-free transmission using current transmission methods [13,17,18,22–24].

Here, we propose a transmission scheme called dual-channel transferring after interference (DCTAI) for fiber-based QIT. The DCTAI scheme takes advantage of the insensitivity of photoelectric detection to the phase and polarization of the optical field, as well as the noise properties of the GAWBS effect. Specifically, the DCTAI scheme settings are as follows: the signal beam is overlapped at

a 50:50 beam splitter with a strong LO, then the output modes are transmitted by two fiber channels. The transmission characteristics and channel capacity can be obtained by measuring the photocurrent difference of the output modes after transmission. We demonstrate this by the QIT of squeezed states, one of the most basic CV quantum states, as an example. Our experimental results demonstrate that the DCTAI scheme effectively eliminates the effect of channel noise, while significantly boosting the channel capacity for CV QIT. Our findings suggest that the full-scale implementation of the DCTAI scheme holds promise for achieving reliable and high-capacity QIT in fiber-based systems.

## II. THE PRINCIPLE AND METHOD

To reduce the difficulty of phase locking between the signal beam and LO in homodyne detection at the receiver’s end, the simultaneous transmission of a perpendicularly polarized signal beam and a LO in a single fiber is a simple and efficient method, known as the PDM. The GAWBS noise scattered by a strong LO is superimposed on the signal field, accelerating the decoherence of quantum states and gradually eliminating their quantum properties in this fiber. GAWBS is a nonlinear phenomenon in fibers; previous research has illuminated the generation mechanism and principle in detail [25–28]. GAWBS can be roughly divided into two types, one of which is the polarized GAWBS caused by the radial-mode ( $R_{0,m}$ ) acoustic waves, which will increase the phase noise of light, and the other is depolarized GAWBS caused by torsional-radial-mode ( $TR_{2,m}$ ) acoustic waves, which are the source of the polarization noise of light [29].

As shown in Fig. 1(a), the output field includes a transferred input quantum state with  $S$  polarization and a  $P$ -polarized thermal state consisting of GAWBS photons from the input state:

$$\hat{a}_S = \sqrt{\eta} \left( \sqrt{1 - \varepsilon_g} \hat{a} + \sqrt{\varepsilon_g} \hat{v} \right) + \sqrt{1 - \eta} \hat{v}, \quad (1)$$

$$\hat{a}_P = \sqrt{\eta \varepsilon_g} \hat{a} + \sqrt{1 - \eta} \hat{v}, \quad (2)$$

where  $\hat{a}$  is the input state;  $\hat{a}_S$  is the output of the  $S$ -polarized input state, which is exploited to measure and obtain the main information on  $\hat{a}$ ;  $\hat{a}_P$  defines the output  $P$ -polarized state caused by GAWBS;  $\eta$  is the total transmission efficiency of the fiber;  $\varepsilon_g$  is the photon-scattering efficiency due to depolarized GAWBS in the fiber; and  $\hat{v}$  represents the vacuum. In addition, the total number of photons outputted by the two channels is  $\hat{a}_S^\dagger \hat{a}_S + \hat{a}_P^\dagger \hat{a}_P = \eta \hat{a}^\dagger \hat{a}$ .

In a Gaussian QIT system based on a fiber channel, the usual PDM transmission scheme can be described as shown in Fig. 1(b). The signal field,  $\hat{s}$ , and the LO,  $\hat{L}$ , are coupled at a polarization beam splitter (PBS) with mutually orthogonal polarizations ( $S$  and  $P$ ), then the coupled

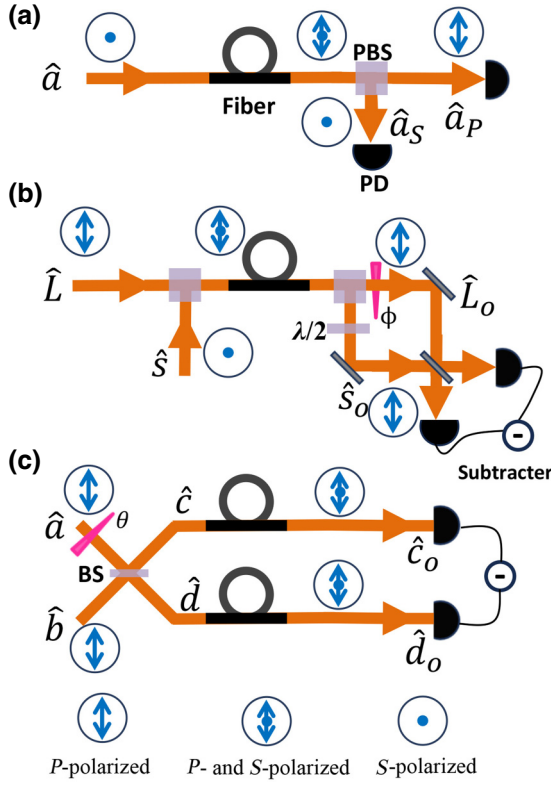


FIG. 1. Sketches of the single-mode fiber transmission (a), usual PDM transmission scheme (b) and DCTAI scheme (c). PD, photodetector;  $\theta$ , phase controller; BS, beam splitter;  $\lambda/2$ , half-wave plate. For clarity, the polarization directions of the light fields are indicated.

field with two polarizations passes through the fiber channel and further decouples on the other PBS. The output signal field,  $\hat{s}_o$ , and the LO,  $\hat{L}_o$ , are

$$\hat{s}_o = \sqrt{\eta} \left( \sqrt{1 - \varepsilon_g} \hat{s} + \sqrt{\varepsilon_g} \hat{L} \right) + \sqrt{1 - \eta} \hat{v}, \quad (3)$$

$$\hat{L}_o = \sqrt{\eta} \left( \sqrt{1 - \varepsilon_g} \hat{L} + \sqrt{\varepsilon_g} \hat{s} \right) + \sqrt{1 - \eta} \hat{v}. \quad (4)$$

As shown in Fig. 1(b), the signal field,  $\hat{s}_o$ , is measured through homodyne detection; the difference current can be expressed as  $i = e^{i\phi} \hat{s}_o^\dagger \hat{L}_o + e^{-i\phi} \hat{L}_o^\dagger \hat{s}_o$ . The LO is a strong coherent state, the scattering efficiency is small enough, and  $|L|^2 \gg |s|^2$ . According to  $|L_o|^2 = \eta |L|^2$ ,  $i$  can be further represented as

$$\begin{aligned} i \approx & \eta \sqrt{1 - \varepsilon_g} |L| \left( e^{i\phi} \hat{s}^\dagger + e^{-i\phi} \hat{s} \right) \\ & + \eta \sqrt{\varepsilon_g} |L| \left( e^{i\phi} \hat{L}^\dagger + e^{-i\phi} \hat{L} \right) \\ & + \sqrt{\eta(1 - \eta)} |L| \left( e^{i\phi} \hat{v}^\dagger + e^{-i\phi} \hat{v} \right), \end{aligned} \quad (5)$$

where the first term is the quadrature component of the signal light,  $\hat{s}$ ; the second term is the quadrature component of

the GAWBS field scattered by the LO,  $\hat{L}$ ; and the third term is vacuum noise introduced by loss. These three items are amplified by the strong LO as effective measurement items.

In Refs. [18,23], the LO optical chopping and time delay can effectively eliminate the GAWBS term [the second term in Eq. (5)], but optical chopping also reduces the communication capacity in the time domain. Therefore, we propose the DCTAI scheme, as shown in Fig. 1(c). This approach may fail in some schemes (such as requiring the separation of the quantum state from the LO after transmission), but succeeds in situations where strict separation of the quantum state and LO is unnecessary (such as quantum secret sharing [19] and QKD systems based on CV entangled states [14,30]). Continuous QIT can further improve the key rate and swapping rate, while ensuring that quantum information is not affected by GAWBS.

Figure 1(c) shows a schematic diagram of the DCTAI scheme. The signal beam,  $\hat{a}$ , and the LO beam,  $\hat{b}$ , are coupled to produce  $\hat{c}$  and  $\hat{d}$  at a 50:50 beam splitter. Then,  $\hat{c}$  and  $\hat{d}$  are simultaneously transmitted through two separate fiber channels as  $\hat{c}_o$  and  $\hat{d}_o$ :

$$\hat{c}_o = \sqrt{\frac{\eta_1}{2}} (\hat{a} + \hat{b} e^{i\theta}) + \sqrt{1 - \eta_1} \hat{v}, \quad (6)$$

$$\hat{d}_o = \sqrt{\frac{\eta_2}{2}} (\hat{a} - \hat{b} e^{i\theta}) + \sqrt{1 - \eta_2} \hat{v}, \quad (7)$$

where  $\theta$  is the relative phase between  $\hat{a}$  and  $\hat{b}$ . When the two channels are the same kind of fiber and there is not much difference in distance, the transmission efficiency of the two channels can be approximately equal, i.e.,  $\eta_1 \approx \eta_2 \approx \eta$ . To facilitate calculations, the light fields are linearized and expressed by the sum of the average term and fluctuation term, for example,  $\hat{a} = \alpha + \delta\hat{a}$  and  $\hat{b} = \beta + \delta\hat{b}$ . According to the requirements of balanced homodyne detection, the intensity of the LO is much greater than that of the signal field, i.e.,  $|\beta|^2 \gg |\alpha|^2$ . The fields  $c_o$  and  $d_o$  are detected by two photodiodes, and the photocurrents are  $I_{c_o} \propto \hat{c}_o^\dagger \hat{c}_o$ , with alternating parts

$$\begin{aligned} i_{c_o} \propto & \frac{\eta}{2} (\beta(\delta\hat{b}^\dagger + \delta\hat{b}) + \beta(\delta\hat{a}^\dagger e^{i\theta} + \delta\hat{a} e^{-i\theta})) \\ & + \frac{\sqrt{\eta(1 - \eta)}}{2} (\beta(\delta\hat{v} e^{-i\theta} + \delta\hat{v}^\dagger e^{i\theta})), \end{aligned} \quad (8)$$

$$\begin{aligned} i_{d_o} \propto & \frac{\eta}{2} (\beta(\delta\hat{b}^\dagger + \delta\hat{b}) - \beta(\delta\hat{a}^\dagger e^{i\theta} + \delta\hat{a} e^{-i\theta})) \\ & - \frac{\sqrt{\eta(1 - \eta)}}{2} (\beta(\delta\hat{v} e^{-i\theta} + \delta\hat{v}^\dagger e^{i\theta})). \end{aligned} \quad (9)$$

The quadrature amplitude and phase of signal field  $\hat{a}$  are  $\hat{Q}_a = \pm(\hat{a}^\dagger + \hat{a})$  and  $\hat{P}_a = \mp i(\hat{a}^\dagger - \hat{a})$ , respectively. When  $\theta = 0, \pi$ , the variance of the alternating difference current

can be given by

$$\langle \delta^2 i \rangle = \eta^2 \beta^2 \delta^2 \hat{Q}_a + \eta(1 - \eta) \beta^2, \quad (10)$$

and if  $\theta = \pm(\pi/2)$ , the result is as follows:

$$\langle \delta^2 i \rangle = \eta^2 \beta^2 \delta^2 \hat{P}_a + \eta(1 - \eta) \beta^2, \quad (11)$$

where  $\langle \delta^2 \hat{X} \rangle = \langle \hat{X}^2 \rangle - \langle \hat{X} \rangle^2$  with  $\hat{X} \in \{\hat{Q}, \hat{P}\}$ , and vacuum noise is normalized to a unit, i.e.,  $\langle \delta^2 \hat{Q}_v \rangle = \langle \delta^2 \hat{P}_v \rangle = 1$ . It can be seen that, due to the lack of a polarization multiplexing method, the DCTAI scheme enables the accurate transmission of both quadratures' information on the transferred quantum state without the GAWBS contributions. As a result, the received state information is only dependent on the transmission efficiency.

However, another challenge lies ahead in the practical implementation of the DCTAI scheme. To extract quantum state information, the two detected signals need to be subtracted. Due to the two spatially separated independent fiber paths, there are inherent losses and a time delay between the two signals, which can impact the accuracy of the difference signal. To address this issue, we conduct experimental measurements of the delay and loss. Fortunately, our measurements show that these parameters are fixed for a constant fiber length. Therefore, appropriate signal postprocessing can be used to compensate for the delay.

### III. EXPERIMENTAL SETUPS

Figure 2 shows the main experimental setup for the DCTAI scheme, which allows for the realization of noiseless and efficient QIT using nonclassical states as well as the estimation of channel capacities. Alice and Bob are designated as the sender and receiver, respectively. Alice's station houses the quantum state generation and transmission devices, where a continuous dual-wavelength Nd:YVO<sub>4</sub>/LiB<sub>3</sub>O<sub>5</sub> laser operating at 671 and 1342 nm serves as the primary light source. To increase intensity stability and implement spatiotemporal filtering, the two lasers pass through a dichroic beam splitter and two separate MCs. The OPA is achieved through a nonlinear periodically poled KTiOPO<sub>4</sub> crystal and a pair of concave mirrors, with ISOs placed between the OPA and MCs to prevent reflected lasers from destabilizing the output of the MC [31]. A 5%-loss ISO is placed after the OPA to prevent light scattering back from the fiber. Scattered light could compromise OPA locking and introduce extra noise to the light-field transmission. The AM loads signals onto the light field, and the BHD system measures amplitude or phase information of the generated squeezed state directly. The fields  $\hat{c}$  and  $\hat{d}$  are then transmitted to Bob through two 3-km single-mode fiber channels with

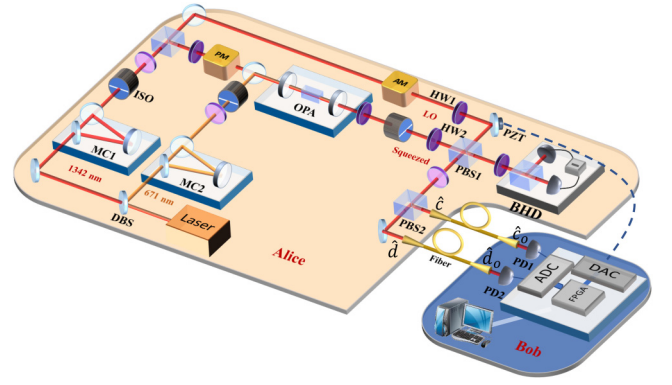


FIG. 2. Experimental setup for implementing information transmission of the squeezed state with the DCTAI scheme. Alice is the sender and Bob is the receiver. DBS, dichroic beam splitter; MC, mode cleaner; ISO, optoisolator; PM, phase modulator; OPA, optical parametric amplifier; PZT, piezoelectric transducer; AM, amplitude modulator; BHD, balanced homodyne detector; HW, half-wave plate; ADC, analog-digital converter; DAC, digital-analog converter.

a loss of 0.35 dB/km, and Bob's measurement and post-processing systems consist of PDs, data acquisition, data processing, and data output. By controlling the piezoelectric transducer and operating the digital-analog converter, the relative phase of the signal and LO can be adjusted.

To compare the performance of the DCTAI scheme with the general PDM scheme, it is necessary to measure the GAWBS noise of the PDM scheme during transmission. The experimental setup for the PDM scheme is shown in Fig. 3. A continuous-wave squeezed state generated from the OPA is combined with the LO on the first PBS using different polarizations. By adjusting the HW, the squeezed light and LO can be controlled to enter measurement system BHD1 for direct measurement or transmitted to BHD2

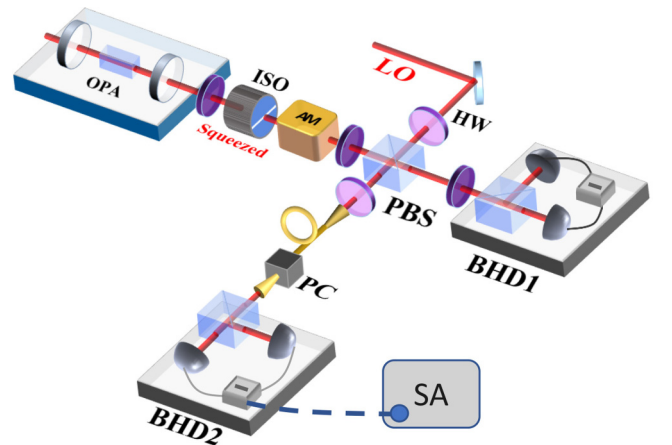


FIG. 3. Experimental setup for measuring channel noise during transmission with the squeezed state in the PDM scheme. PC, polarization controller; SA, spectrum analyzer.

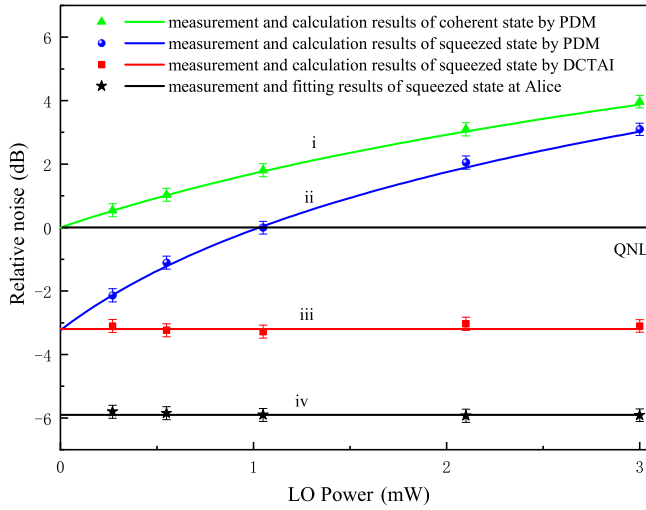


FIG. 4. Effect of polarized GAWBS noise on squeezed state with the PDM and DCTAI schemes. Measured and calculated results of quantum noise level vary with the LO power when the length of the fiber is 3 km. Curves and symbols are the theoretical and experimental results, respectively.

through a 3-km single-mode optical fiber for further analysis. At the receiver, the signal interferes with the LO on the PBS of BHD2 by controlling the polarization controller and the light-field noise is measured with BHD2 and a spectrum analyzer.

With the experimental setup shown in Fig. 3, we measured the GAWBS noise spectrum of TR mode with a 3-km fiber and 3-mW incident LO, see the Appendix. Then the quantum state transmission is determined by PDM. Since the GAWBS noise increases linearly with the LO power, we measure the transmission characteristics of quantum states under different LO powers. The triangles in Fig. 4 show the polarized GAWBS noise when the LO power is 0.27, 0.55, 1.05, 2.1, and 3.0 mW, and trace (i) corresponds to the calculation result with the coherent state. The circles and trace (ii) represent the measured and calculated output noise level for the squeezed state with the PDM scheme, respectively, indicating that GAWBS noise seriously destroys quantum states during PDM transmission.

#### IV. ELIMINATION OF CHANNEL NOISE WITH THE DCTAI SCHEME

To verify the immunity of the DCTAI transmission scheme to GAWBS noise, experiments have been conducted using the setup shown in Fig. 2. First, to eliminate the error caused by different delays and losses, the two fiber channels need to be calibrated. The main method used in this study is as follows. A periodic amplitude-modulation signal is added to the LO at the input port of a fiber, which

is then transmitted over two fiber channels for calibration. The outputs are measured by PD1 and PD2, and data are acquired by high-speed low-delay ADCs. The loss and relative delay of the two channels are obtained by an field programmable gate array (FPGA) program and added to the subsequent signal processing to compensate for the error caused by the different distances between the two channels.

Next, we measure the squeezed state generated from OPA using BHD1, and obtain a squeezed noise level of 5.9 dB below the standard quantum limit (SQL) at 2 MHz, as shown in Fig. 4(iv). By adjusting the settings of HW1 and HW2 (as shown in Fig. 2), we change the signal and LO to the transmission mode. After passing through PBS2, the fields  $\hat{c}$  and  $\hat{d}$  are transmitted through two fiber channels, respectively, and the quadratures of the transferred quantum state can be measured by controlling the relative phase of the signal field and LO using a piezoelectric transducer. The measured squeezing values subsequent to transmission are depicted by squares in Fig. 4 and remain approximately constant at  $-3.2$  dB, despite varying levels of LO power (i.e., different GAWBS noise levels). Trace (iii) represents the theoretical result of the quantum state when only the loss is considered, according to Eq. (10), which is in perfect agreement with the measurements. The results show that, in contrast to PDM, both experimental and theoretical results demonstrate that the influence of GAWBS noise on quantum states can be completely eliminated using the DCTAI scheme, and only fiber loss affects the signal fields during remote transmission. This is a significant advantage in QIT.

#### V. IMPROVEMENT OF SENSITIVITY IN MEASURING GAWBS NOISE WITH THE SQUEEZED STATE

Additionally, the measurement sensitivity of the polarized GAWBS noise in an optical fiber is improved with the help of the squeezed state. Normally only the input LO is needed to measure the GAWBS noise of that LO. In this case, the measured GAWBS noise level is based on vacuum noise, and the measured signal-to-noise ratio (SNR) can be represented as the gap between the green curve and the quantum noise limit (QNL) in Fig. 4. The sensitivity of measuring GAWBS noise can be improved by introducing a squeezed light, which means that the squeezed light and LO are transmitted simultaneously in a single fiber with different polarizations. On this occasion, the GAWBS noise measured is based on the squeezed vacuum noise, and the measured SNR corresponds to the gap between the blue and red curves, as shown in Fig. 4. The results show that, under our experimental conditions, the SNR of polarized GAWBS noise measured using the squeezed state is 6.2 dB when the LO power is 3 mW, which is 2.3 dB better than the direct measurement.

## VI. IMPROVING THE COMMUNICATION CAPACITY THROUGH THE DCTAI SCHEME

Finally, we compare the channel capacity of the DCTAI, PDM, and PTDM schemes in the frequency range of 1–10 MHz at 3-mW LO. Detailed information about the PTDM scheme can be found in Ref. [18]. In this experiment, the LO pulse can be obtained via AM, as shown in Fig. 3, and the PTDM scheme can be realized by introducing a time delay (not shown in Fig. 3) in the LO optical path after fiber transmission. We measure the channel noise and estimate the communication capacity with the squeezed or coherent state as a carrier under the condition of the same modulated signal using the three schemes, as well as the ideal case without noise and loss. The modulated signal is white Gaussian noise and increases the coherent-state noise by 3 dB, ranging from 1 to 10 MHz. Based on the measurement signal, noise levels, and Shannon's formula [ $C = W \times \log_2(1 + S/N)$ , where  $C$  is the channel capacity,  $W$  is the bandwidth,  $S$  is the signal power, and  $N$  is the noise power], we obtain the normalized channel capacities, as shown in Fig. 5. Limited by the transmission pattern of the OPA, the squeezing degree of the squeezed state decreases as the frequency increases, dropping to 1.9 dB at 10 MHz.

In the PTDM scheme, two types of pulsed LO with high and low repetition rates are adopted, as mentioned in Ref. [18]. The repetition rates are 8 and 0.5 MHz, respectively, with the same duty cycle of 30%. In the experiments, we used different schemes and different carriers but identical modulated signals. Traces (i)–(iii) in Fig. 5(a) show measurement results using the squeezed light as the carrier, while the other traces in Fig. 5(b) use the coherent light as the carrier. Traces (i) and (iv) represent the channel capacity per unit bandwidth through the ideal transmission channel without noise and loss. Then, using the DCTAI scheme, the channel capacity per unit

bandwidth refers to traces (ii) and (v), while PDM refers to traces (iii) and (vi), and PTDM refers to traces (vii) and (viii).

Figure 5 clearly shows that the DCTAI scheme based on the squeezed carrier light achieves the highest channel capacity. When the squeezing degree is  $-5.9$  dB, the channel capacity per unit bandwidth is about 1.25 bits/(s Hz), which is higher than the classical limit. Moreover, the channel capacity of the DCTAI scheme is significantly higher than that of other schemes with the same carrier case.

## VII. CONCLUSION

We propose and demonstrate a practical method for QIT via fiber channels called the DCTAI scheme. Significantly, what we transmit is a mixed mode of a signal field and LO that is easy to transmit and measure, rather than a complete quantum state, since the output quantum state at the end of the fiber cannot be separated from the output field. However, quadrature information about the input quantum state can be obtained through direct intensity measurements. Therefore, we claim that this is a QIT scheme. In this scheme, the fiber channel serves as part of homodyne detection and does not contribute GAWBS noise to the measurement results, nor does it require the use of a pulsed LO with a smaller capacity like PTDM. Two main experiments were conducted to validate this approach. Based on the DCTAI scheme, the impact of GAWBS noise and phase noise on the transmitted information is minimal, with transmission mainly limited by fiber loss. Incidentally, we improved the sensitivity of measuring GAWBS noise introduced by a strong LO using squeezed light.

Moreover, the DCTAI scheme can provide more complete and continuous quantum information, in both time and frequency domains, resulting in a higher communication capacity compared to PTDM and PDM. It should be noted that errors due to channel independence can be resolved by calibrating channel delay and loss, as well as postprocessing the collected information, which removes a major obstacle to practical application. Therefore, due to the characteristics of high bandwidth, low noise, and large capacity, the DCTAI scheme has the potential to construct deterministic quantum communication networks.

Finally, the question of the applicability of this transmission scheme needs to be discussed. The proposed QIT scheme is suitable for many long-distance CV quantum communication schemes, including quantum secret sharing, QKD, and quantum entanglement swapping based on the entangled state. As for quantum dense encoding and quantum teleportation, it may be useless. For example, for quantum secret sharing based on bound states, the dealer can transmit secret information and LO light to several remote sharing users, according to the transmission scheme here, and these remote users cooperate

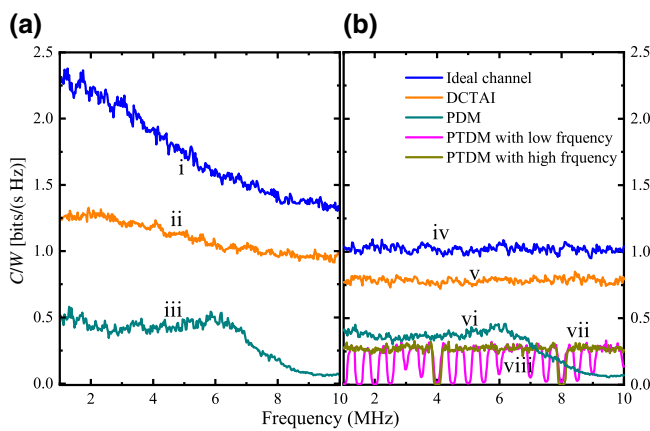


FIG. 5. Measurement results of channel capacity per unit bandwidth. (a),(b) Results of squeezed and coherent states, respectively, with shared legends and coordinates.

for decryption. However, for dense encoding based on entangled states, this is not applicable because the information loading and sending of entangled submodes must be completed at the same end, that is, the sending end. To ensure the security of the entangled submode for demodulation, the entangled state is generally prepared by the receiver. In fact, due to the signal-LO coupling before transmission, the input quantum state cannot be separated at the end of fiber-optic transmission, which determines that the proposed scheme can only be applied to these unmodulated CV quantum information protocols.

Data that support the findings of this study are available from the corresponding author upon reasonable request.

### ACKNOWLEDGMENTS

This work was supported by the National Natural Science Foundation of China (Grants No. 61925503, No. 62122044, and No. 62135008), the Key Project of the National Key R&D program of China (Grant No. 2022YFA1404500), the Program for the Innovative Talents of the Higher Education Institutions of Shanxi, the Program for the Outstanding Innovative Teams of the Higher Learning Institutions of Shanxi, the Fund for Shanxi “1331 Project” Key Subjects Construction, and the Applied Basic Research Project of Shanxi Province (202203021212481).

### APPENDIX: THE POLARIZED GAWBS NOISE LEVELS IN A FIBER CHANNEL WITH A LO POWER OF 3 MW

With the experimental setup shown in Fig. 3 in the main text, we measure the GAWBS noise spectrum of TR mode within 1 GHz and 10 MHz, where the length of the optical

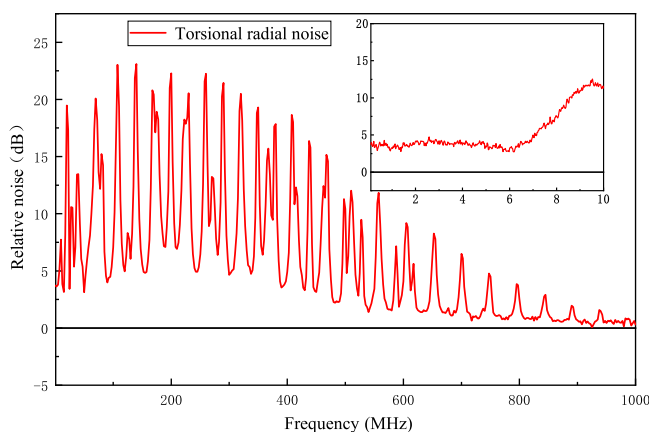


FIG. 6. Polarized GAWBS noise levels measured at the output field of a fiber within 1 GHz and 10 MHz. Measurement parameters are as follows for the spectrum analyzer: resolution bandwidth, 100 kHz; video bandwidth, 100 Hz. Inset shows the polarized GAWBS noise level within 10 MHz.

fiber is 3 km and the power of the incident LO is 3 mW. The normalized results are shown in Fig. 6, where the level of 0 dB corresponds to the SQL. As illustrated in the figure, polarized GAWBS noise is consistently present within the 1-GHz bandwidth and exhibits a more than 3-dB excess over the SQL within the 10-MHz frequency range.

- [1] N. Sangouard, C. Simon, H. de Riedmatten, and N. Gisin, Quantum repeaters based on atomic ensembles and linear optics, *Rev. Mod. Phys.* **83**, 33 (2011).
- [2] Y. Guo, Q. Liao, D. Huang, and G. Zeng, Quantum relay schemes for continuous-variable quantum key distribution, *Phys. Rev. A* **95**, 042326 (2017).
- [3] H. Takenaka, A. Carrasco-Casado, M. Fujiwara, M. Kitamura, M. Sasaki, and M. Toyoshima, Satellite-to-ground quantum-limited communication using a 50-kg-class microsatellite, *Nat. Photonics* **11**, 502 (2017).
- [4] B. Korzh, C. C. W. Lim, R. Houlmann, N. Gisin, M. J. Li, D. Nolan, B. Sanguinetti, R. Thew, and H. Zbinden, Provably secure and practical quantum key distribution over 307 km of optical fibre, *Nat. Photonics* **9**, 163 (2015).
- [5] S. Wang, Z.-Q. Yin, D.-Y. He, W. Chen, R.-Q. Wang, P. Ye, Y. Zhou, G.-J. Fan-Yuan, F.-X. Wang, W. Chen, Y.-G. Zhu, P. V. Morozov, A. V. Divochiy, Z. Zhou, G.-C. Guo, and Z.-F. Han, Twin-field quantum key distribution over 830-km fibre, *Nat. Photonics* **16**, 154 (2022).
- [6] J. Bogdanski, N. Rafiei, and M. Bourennane, Experimental quantum secret sharing using telecommunication fiber, *Phys. Rev. A* **78**, 062307 (2008).
- [7] A. Furusawa, J. L. Sørensen, S. L. Braunstein, C. A. Fuchs, H. J. Kimble, and E. S. Polzik, Unconditional quantum teleportation, *Science* **282**, 706 (1998).
- [8] M. Huo, J. Qin, J. Cheng, Z. Yan, Z. Qin, X. Su, X. Jia, C. Xie, and K. Peng, Deterministic quantum teleportation through fiber channels, *Sci. Adv.* **4**, eaas9401 (2018).
- [9] J. Lodewyck, T. Debuisschert, R. Tualle-Brouri, and P. Grangier, Controlling excess noise in fiber-optics continuous-variable quantum key distribution, *Phys. Rev. A* **72**, 050303(R) (2005).
- [10] E. Ip and J. Kahn, Feedforward carrier recovery for coherent optical communication, *J. Lightwave Technol.* **25**, 2675 (2007).
- [11] Z. Fang, H. Cai, G. Chen, and R. Qu, in *Single Frequency Semiconductor Lasers* (Springer, Singapore, 2017), p. 235.
- [12] A. C. Bordonalli, Optical injection phase-lock loops. Ph.D. University College London, 1996.
- [13] B. Qi, P. Lougovski, R. Pooser, W. Grice, and M. Bobrek, Generating the local oscillator “locally” in continuous-variable quantum key distribution based on coherent detection, *Phys. Rev. X* **5**, 041009 (2015).
- [14] N. Wang, S. Du, W. Liu, X. Wang, Y. Li, and K. Peng, Long-distance continuous-variable quantum key distribution with entangled states, *Phys. Rev. Appl.* **10**, 064028 (2018).
- [15] J. Lodewyck, T. Debuisschert, R. García-Patrón, R. Tualle-Brouri, N. J. Cerf, and P. Grangier, Experimental

- implementation of non-gaussian attacks on a continuous-variable quantum key distribution system, *Phys. Rev. Lett.* **98**, 030503 (2007).
- [16] B. Qi, L.-L. Huang, L. Qian, and H.-K. Lo, Experimental study on the Gaussian-modulated coherent-state quantum key distribution over standard telecommunication fibers, *Phys. Rev. A* **76**, 052323 (2007).
- [17] Q. D. Xuan, Z. S. Zhang, and P. L. Voss, A 24 km fiber-based discretely signaled continuous variable quantum key distribution systems, *Opt. Express* **17**, 24244 (2009).
- [18] J. Qin, J. Cheng, S. Liang, Z. Yan, X. Jia, and K. Peng, Transferring of continuous variable squeezed states in 20 km fiber, *Appl. Sci.* **9**, 2397 (2019).
- [19] Y. Zhou, J. Yu, Z. Yan, X. Jia, J. Zhang, C. Xie, and K. Peng, Quantum secret sharing among four players using multipartite bound entanglement of an optical field, *Phys. Rev. Lett.* **121**, 150502 (2018).
- [20] X. Jia, X. Su, Q. Pan, J. Gao, C. Xie, and K. Peng, Experimental demonstration of unconditional entanglement swapping for continuous variables, *Phys. Rev. Lett.* **93**, 250503 (2004).
- [21] X. Su, C. Tian, X. Deng, Q. Li, C. Xie, and K. Peng, Quantum entanglement swapping between two multipartite entangled states, *Phys. Rev. Lett.* **117**, 240503 (2016).
- [22] I. Suleiman, J. A. H. Nielsen, X. Guo, N. Jain, J. S. Neergaard-Nielsen, T. Gehring, and U. L. Andersen, 40 km fiber transmission of squeezed light measured with a real local oscillator, *Quantum Sci. Technol.* **7**, 045003 (2022).
- [23] T. Wang, P. Huang, Y. Zhou, W. Liu, H. Ma, S. Wang, and G. Zeng, High key rate continuous-variable quantum key distribution with a real local oscillator, *Opt. Express* **26**, 2794 (2018).
- [24] B. Huang, Y. Huang, and Z. Peng, Practical security of the continuous-variable quantum key distribution with real local oscillators under phase attack, *Opt. Express* **27**, 20621 (2019).
- [25] R. M. Shelby, M. D. Levenson, and P. W. Bayer, Guided acoustic-wave Brillouin scattering, *Phys. Rev. B* **31**, 5244 (1985).
- [26] R. M. Shelby, M. D. Levenson, and P. W. Bayer, Resolved forward Brillouin scattering in optical fibers, *Phys. Rev. Lett.* **54**, 939 (1985).
- [27] D. Elser, U. L. Andersen, A. Korn, O. Glöckl, S. Lorenz, Ch. Marquardt, and G. Leuchs, Reduction of guided acoustic wave Brillouin scattering in photonic crystal fibers, *Phys. Rev. Lett.* **97**, 133901 (2006).
- [28] N. Hayashi, Y. Mizuno, K. Nakamura, S. Y. Set, and S. Yamashita, Experimental study on depolarized GAWBS spectrum for optomechanical sensing of liquids outside standard fibers, *Opt. Express* **25**, 2239 (2017).
- [29] Y. M. Li, N. Wang, X. Y. Wang, and Z. L. Bai, Influence of guided acoustic wave Brillouin scattering on excess noise in fiber-based continuous variable quantum key distribution, *J. Opt. Soc. Am. B* **31**, 2379 (2014).
- [30] S. Du, Y. Tian, and Y. Li, Impact of four-wave-mixing noise from dense wavelength-division-multiplexing systems on entangled-state continuous-variable quantum key distribution, *Phys. Rev. Appl.* **14**, 024013 (2020).
- [31] M. Huo, J. Qin, Z. Yan, X. Jia, and K. Peng, Generation of two types of nonclassical optical states using an optical parametric oscillator with a PPKTP crystal, *Appl. Phys. Lett.* **109**, 221101 (2016).